https://doi.org/10.5194/egusphere-2026-3696
Preprint. Discussion started: 2 July 2026

Resolving agroforestry extent with a sub-meter tree map and high-resolution land-use data across Europe and the Sahel

Ouadya Tahiri[1], Damien Beillouin[2], Patrice Dumas[3], Rémi Prudhomme[3], David Makowski[4]

[1]AgroParisTech, UMR CIRED, Palaiseau 91120, France
[2]CIRAD, UPR HORTSYS, Montpellier, France
[3]CIRAD, UMR CIRED, F-34398 Montpellier, France
[4]Université Paris-Saclay, AgroParisTech, INRAE, UMR 518 MIA-PS, Palaiseau 91120, France

Correspondence to: Ouadya Tahiri (ouadya.tahiri@agroparistech.fr)

Abstract. Global agroforestry maps remain uncertain, partly because agricultural land masks used to identify farmland trees have never been systematically validated against ground-truth data. Existing approaches rely on coarse-resolution land-use products and discrete classifications that poorly capture the continuum of tree–crop integration, directly affecting large-scale estimates of climate mitigation and ecosystem services provided by agroforestry. Here, we present the first systematic evaluation of how different land-use masks affect agroforestry mapping accuracy, combining agricultural land masks derived from three 10-meter land-use/land-cover products with a global sub-meter resolution tree canopy map. Validating each land mask-tree canopy combination against 14,162 georeferenced ground-truth observations that distinguish agroforestry from non-agroforestry trees, we find that the choice of agricultural land mask alone drives a 45-percentage-point shift in accuracy. The ESRI-based mask achieves 77.2% accuracy, outperforming ESA WorldCover (69%), Dynamic World (68%), and the Global Pasture Watch (GPW)- based map (32%) across all biomes tested. Applying the best-performing combination, we estimate that 86 million hectares of agricultural land in Europe and 36 million hectares in the Sahel host at least 1% tree cover, with sparse-canopy systems (<10% tree cover) dominating both regions (32 Mha and 21 Mha, respectively). These estimates diverge sharply from the most cited agroforestry maps, which overestimate agroforestry extent by up to 186% in Europe and underestimate it by 80% in the Sahel. Together, these findings demonstrate that both land-use mask selection and tree-detection resolution are major, previously unquantified sources of uncertainty in global agroforestry assessments, and call for a shift away from coarse-resolution gridded data toward tree-centric, gradient-based approaches capable of resolving individual trees across the agriculture–forest continuum.

https://doi.org/10.5194/egusphere-2026-3696
Preprint. Discussion started: 2 July 2026

1 Introduction

Agroforestry systems (AFS), the intentional integration of trees with crops and/or livestock on the same land management unit, are practiced worldwide under diverse forms (Nair, 1993) and represent one of the largest agricultural Natural Climate Solutions (Terasaki Hart et al., 2023). Beyond climate mitigation and carbon sequestration (Cardinael et al., 2018), agroforestry supports biodiversity conservation (Jones et al., 2021), improves water quality (Zhu et al., 2020), and, under certain conditions, can increase food production (Beillouin et al., 2021; Ivezić et al., 2021). Yet, despite this recognized potential, significant uncertainty surrounds the current and potential AFS extent, leading to even higher uncertainties in its contribution to climate mitigation and ecosystem services.

Global estimates of agroforestry extent diverge by nearly a factor of four, from 400 Mha (IPCC, 2000) to 1,600 Mha (Nair, 2012), depending on definitions, data sources, and mapping approaches. Intermediate estimates converge around 700 Mha (Lesiv et al., 2022) to 859 Mha (Zomer et al., 2014, 2022). These discrepancies contribute to the uncertainty in agroforestry biomass stocks, which range between 10 PgC of carbon (Zomer et al., 2016) for all agroforestry forms, to 3.07-3.86 PgC for woody biomass on croplands and pastures (Chapman et al., 2020). Such variability in both area and carbon estimates highlights that current global assessments of agroforestry mitigation potential are highly sensitive to the methodological choices in land use mapping and classification.

Mapping AFS at large scales is challenged by the absence of a universally shared operational definition of agroforestry. In practice, two elements of the agroforestry definition are often ignored: *intentionality* (the deliberate integration of trees by land managers), which cannot be directly observed, and the combination of trees and crops or livestock in the same management unit, which cannot easily be observed using remote sensing. As a result, at large scales, agroforestry is operationally defined more simply as the presence of trees on croplands and pastures. AFS mapping is also constrained by limited availability of reliable data to assess the uncertainty associated with current maps. Lastly, agroforestry is not a distinct land use type, but rather occupies a continuum between agriculture and forest. Because of this diversity of tree density in agroforestry systems, it is inherently difficult to delineate clear spatial and temporal boundaries for agroforestry systems.

Different approaches have emerged to map and estimate the extent of agroforestry at large scales. The first approach estimates the extent by estimating the probability of agroforestry per country using georeferenced field surveys, such as LUCAS data (Den Herder et al., 2017; Rubio-Delgado et al., 2023). This method is limited by the cost of field surveys, which in turn limits the feasibility and sampling density. The second approach relies on machine learning-based land-use classification (Bolívar-Santamaría and Reu, 2021; Lesiv et al., 2022), in which agroforestry is treated as a distinct land use class with specific spectral signatures. Expert-labelled training data are used to translate conceptual definitions into ground-truth classes, which are then extrapolated across space. While this approach can capture complex patterns locally, its application at continental or global scales is limited by high computational demands, the scarcity of representative training data across diverse

https://doi.org/10.5194/egusphere-2026-3696
Preprint. Discussion started: 2 July 2026

agroforestry systems, and spectral overlap with forests and croplands that can reduce classification accuracy (Sharma et al., 2022).

A third method, more widely adopted, consists of combining a tree cover dataset with an agricultural land mask derived from a land use/land cover (LULC) product (Chapman et al., 2020; Diouf, 2025; Zomer et al., 2009, 2014). While this approach aligns closely with core principles of trees-crop or tree-livestock integration, existing implementations reveal critical limitations along three tightly coupled dimensions: the spatial resolution and definition of agricultural masks (Lillesand et al., 2015), the accuracy of tree cover detection, and the limited validation of the final combination products. First, coarse-resolution of LULC data used to delineate agricultural areas can introduce "mixed pixel" effects, leading to overestimation of agroforestry extent. For instance, a 1 km² pixel with 50% tree cover may represent dense forest adjacent to treeless cropland rather than an integrated agroforestry system, a problem particularly pronounced in fragmented landscapes such as the European Union (Den Herder et al., 2017). Second, widely used global tree-cover datasets, such as the 30 m Hansen et al. (2013) dataset, were designed for closed-canopy forests and underestimate tree cover by up to 80% in heterogeneous European landscapes, missing scattered or low-density trees (<10%cover) (Reiner et al., 2023). Third, the application of strict thresholds to operationally define agroforestry - excluding agricultural land cover below 10% (Zomer et al., 2014) or above 25% (Chapman et al., 2020)- can distort the true distribution of agroforestry, omitting both sparse dryland systems and dense woody perennial systems like coffee plantations or dense alley cropping (Terasaki Hart et al., 2023).

Recent advances in very high-resolution (VHR) remote sensing have substantially improved the detection of individual trees outside forests at national and regional scales (Brandt et al., 2020; Liu et al., 2023; Mugabowindekwe et al., 2023; Reiner et al., 2023). However, a critical source of uncertainty remains largely unaddressed: the choice of agricultural masks used to define where trees are considered “on farms.” Differences among LULC products strongly affect agricultural masks, with direct consequences for estimated agroforestry extent estimates and inferred climate mitigation potentials. Here we address these limitations by: i) combining a sub-meter tree canopy cover map with multiple LULC products, ii) rigorously validating these combinations using a large dataset, and iii) applying the best-performing combination canopy-LULC to estimate the extent of agroforestry systems in two contrasting regions: Europe and the Sahel, comparing the results with existing estimates (Chapman et al., 2020; Lesiv et al., 2022; Zomer et al., 2014). We hypothesize that detecting trees at sub-meter resolution coupled with a precise delineation of agricultural land improves large-scale estimates of agroforestry extent.

https://doi.org/10.5194/egusphere-2026-3696
Preprint. Discussion started: 2 July 2026

2 Material and methods

2.1- Land use and land cover (LULC) data

We define an agroforestry tree as any tree or shrub taller than 1 m present within croplands or pastures under human management. Because any tree present on these land-uses can influence surrounding agricultural processes (positively or negatively), all tree cover ranges (1–100%) are considered, capturing the full spectrum of agroforestry systems. We excluded urban trees, trees in strictly protected areas (categories Ia, Ib, and III) (UNEP-WCMC, 2019)), forest trees (i.e., not interacting with agricultural lands) as well as trees on unmanaged rangelands and grasslands.

Agroforestry maps were produced using four sources: global cropland and pasture maps, a terrestrial human footprint map (to distinguish pastures harvested or grazed by livestock from unmanaged grasslands), and a VHR tree canopy map.

2.1.1- Agricultural masks

Previous agroforestry mapping efforts (Zomer et al., 2009, 2014) were limited by coarse-resolution LULC data, which reduce precision in land-use delineation. Recent advances have yielded three high-resolution (10 m) land use and land cover (LULC) products, offering improved delineation of agricultural land. i) The ESRI Land Cover map employs a Convolutional Neural Network (U-Net model) trained on billions of human-labeled pixels, and achieves an overall accuracy of 85% (Karra et al., 2021). ii) The ESA WorldCover product utilizes a random forest classification based on 131 features from Sentinel-2 multi-spectral imagery and Sentinel-1 C-band Synthetic Aperture Radar (SAR) data, and reaches a global overall accuracy of 74.4% (Zanaga et al., 2022). iii) Dynamic World is based on a Fully Convolutional Neural Network (FCNN) trained on data similar to ESRI's, and achieves 73.8% overall accuracy (Brown et al., 2022).

The high-resolution LULC maps include a dedicated cropland class. For grasslands and rangelands, we selected herbaceous vegetation categories, alongside shrublands, based on land-use category definitions (Table 1). The LULC maps fail to distinguish managed pastures from natural grasslands, a key distinction for silvopastoral systems. To address this, we used the terrestrial Human Footprint Index (HFI) as a spatial proxy for management. This validated 100 m dataset quantifies anthropogenic pressure (scale 0–50) based on infrastructure and population variables (Gassert et al., 2023).

Grasslands and rangelands were classified as pastoral when HFI > 4, a threshold that separates 'low-disturbance' landscapes from those with sufficient human presence to support livestock management (Gassert et al., 2023; Williams et al., 2020).

For comparison, we constructed alternative agricultural masks by integrating the Global Pasture Watch (GPW) dataset (Table1) with the cropland classes from each LULC product. GPW identifies managed grasslands using a 30m resolution Random Forest classifier and explicitly separates managed pastures from natural ecosystems (Parente et al., 2024). Substituting HFI-derived pasture with GPW's layers allowed us to assess sensitivity to managed pasture definitions.

2.1.2-Global tree canopy map

We used the global sub-meter global tree height map developed by Tolan et al. (2024), which provides tree-level information at unprecedented spatial resolution. The dataset combines self-supervised vision transformers

https://doi.org/10.5194/egusphere-2026-3696
Preprint. Discussion started: 2 July 2026

trained on 18 million global satellite images with a convolutional decoder calibrated using airborne lidar data and GEDI spaceborne observations. Derived from Maxar Vivid2 mosaic RGB imagery at 0.59m resolution (2017-2020), the model achieves robust tree segmentation performance (user's accuracy: 0.82; producer's accuracy:0.76).

Unlike previous 10- 30 m products, this dataset resolves individual tree canopy and height in heterogeneous and low-density landscapes, including drylands where scattered trees dominate agroforestry systems. Other datasets (Liu et al., 2023; Mugabowindekwe et al., 2023; Reiner et al., 2023) were not used because of their limited spatial coverage and/or their coarser resolutions. To derive a tree canopy map, we retained pixels with canopy height higher than 1 meter, capturing both shrubs and small trees. This corresponds to the validated segmentation limit of the original model (Tolan et al., 2024)

2.2- Data processing

2.2.1- Time series data reduction

We filtered all LULC datasets to retain relevant classes for agroforestry (croplands, rangelands, grasslands, and shrublands). To reduce temporal noise caused by cloud coverage and algorithmic variability, thereby obtaining a more representative and stable land use classification, we aggregated multi-year LULC products using the modal reducer in Google Earth Engine, assigning each pixel its most frequent class over the period 2017–2024, which corresponds to the period where ESRI and DW, and GPW are all available. For the ESA WorldCover product, available for 2020 and 2021, we retained only the 2021 product as it's more accurate (Zanaga et al., 2022).

2.2.2- Datasets overlaying

We intersected the 1m tree canopy map with cropland and pasture layers to generate spatially explicit agroforestry maps. Tree canopy was overlaid with cropland layers from ESRI, ESA, and DW, and with pasture layers derived either from the same sources or from GPW. For ESRI, DW, and ESA, pasture layers were filtered using the Human Footprint Index (HFI).

This resulted in six agroforestry maps based on two approaches. First, three "single-source" datasets were generated by combining cropland and pasture classes from the same land-use/land-cover (LULC) product (ESRI, ESA, and DW) with the tree canopy map and the HFI filter. Second, three "hybrid" datasets were produced by pairing cropland layers from each LULC product with pasture data from GPW (ESRI-GPW, ESA-GPW, and DW-GPW).

To ensure spatial consistency, all coarser resolution inputs (10m -30m) were resampled to 1m and reprojected to match the tree canopy map. All overlaying operations were conducted in Google Earth Engine (Gorelick et al., 2017) via its Python API, enabling scalable cloud-based computation. All datasets are publicly available within the GEE cloud, ensuring transparency and reproducibility.

2.3- Accuracy assessment

2.3.1 - Validation dataset

We evaluated the accuracy of the six generated 1 m-resolution datasets at a global scale by assessing their ability to correctly identify agroforestry systems while excluding non-agroforestry tree cover (i.e., forests and woody

https://doi.org/10.5194/egusphere-2026-3696
Preprint. Discussion started: 2 July 2026

monocrops). Because no spatially explicit field-based global agroforestry inventory exists, we constructed a composite validation dataset by integrating two independent sources: agroforestry presence was derived from Tahiri et al. (2026) and non-agroforestry tree cover was derived from Lesiv et al. (2022). Tahiri et al. 2026) provide presence data stratified by WWF biomes (Olson et al., 2001), utilizing a 30 m × 30 m observation unit. Based on photo-interpretation of very high resolution (VHR) satellite imagery, this dataset distinguishes woody monocrops from three agroforestry systems: alley cropping (linear rows with inter-tree space), hedgerows (linear tree line less than 20m wide), and scattered trees (e.g., agroforestry parklands). To represent non-agroforestry tree cover, we used the observations labeled as 'woody monocrops' from the same database (Tahiri et al., 2026), and incorporated reference points from (Lesiv et al., 2022), specifically the classes *'Naturally regenerating forest without any signs of human activities'* and *'Planted forests'*. These classes served as negative control points to evaluate the capacity of each map to correctly exclude non-agroforestry tree cover. The total number of data is 14,162 (Fig. 1).

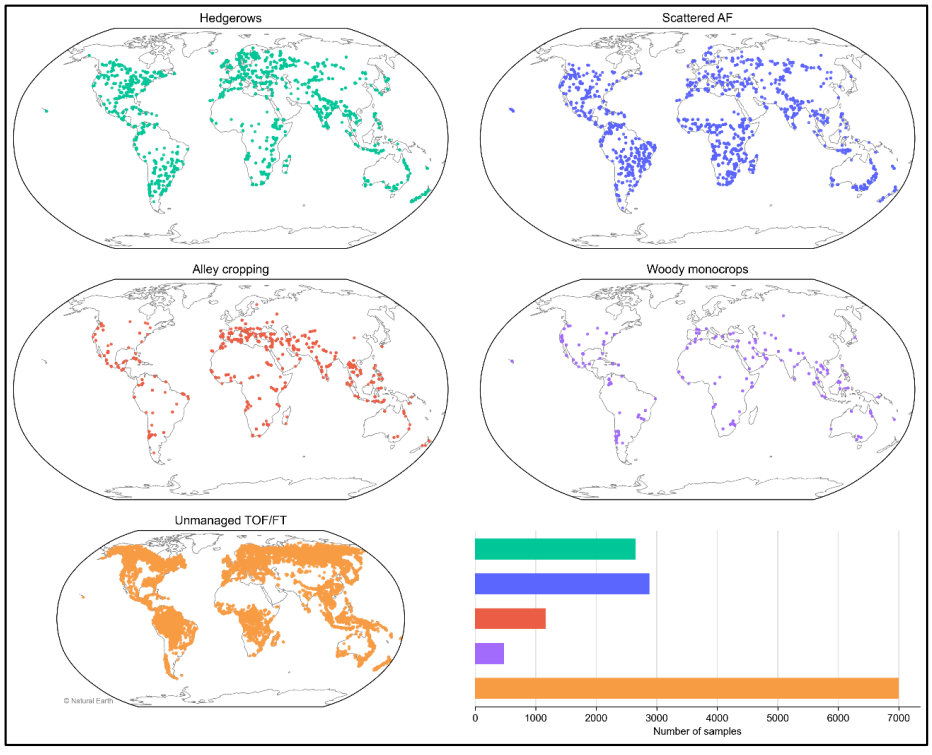

Figure 1: Distribution of the collected reference data used for validation, classified between hedgerow trees, scattered agroforestry trees, alley cropping trees, woody monocrops, and unmanaged trees outside forest (TOF) / forest trees (FT).

https://doi.org/10.5194/egusphere-2026-3696
Preprint. Discussion started: 2 July 2026

2.3.2 - Accuracy metrics

Map accuracy was evaluated by spatially comparing the six agroforestry maps with the georeferenced validation dataset. Reference observation units are defined at 30 m x 30 m, while the generated agroforestry tree maps have a 1m resolution. Each reference observation unit is labelled as *agroforestry* if at least one tree canopy pixel is present within the 30 m × 30 m observation unit, and as *non-agroforestry* otherwise. These map-derived AF predictions were then compared to reference data labels to quantify agreement.

We generated two types of analysis based on confusion matrices. First, a standard 2 × 2 confusion matrix was computed at the observation unit level, from which we calculated Sensitivity (Producer's Accuracy; True Positive (TP) / (TP + False Negative (FN))), measuring the capacity to correctly identify agroforestry, and Specificity (True Negative / (True Negative + False Positive (FP))), measuring the proportion of non-agroforestry sites correctly excluded. Second, a 5 × 2 confusion matrix was constructed to evaluate the ability of each map to identify different agroforestry and non-agroforestry tree cover types. This matrix allows identification of the specific types of classification errors in the agroforestry maps.

To assess performance across biomes, we computed the F1-score, defined as the harmonic mean of precision and recall (Christen et al., 2024). We prioritized the F1 score over overall accuracy because agroforestry is unevenly distributed across biomes, leading to class imbalance, which can bias overall accuracy. Precision was calculated as TP / (TP + FP) and recall as TP / (TP + FN), yielding:

$$F1 - score = 2 . \frac{Precision . Recall}{Precision + Recall}$$

227 Table 1. Definition and resolution of the croplands and grasslands / rangelands from ESRI, ESA, DW and GPW

LULC product	Croplands definition	Grasslands/shrublands / rangelands definition	Spatial resolution (m)	Temporal resolution	Reference
ESRI	Crops Human-planted/plotted cereals, grasses, and crops not at tree height; examples: corn, wheat, soy, fallow plots of structured land	Open areas dominated by homogenous grasses or scattered vegetation with minimal tall plants, including natural meadows, sparse savannas, parks, and pastures, which support activities like grazing, conservation, and recreational uses such as golfing	10m x10m	Annual from 2017 to 2023	(Karra et al., 2021)
ESA	Land covered with annual cropland that is sowed/planted and harvestable at least once within the 12 months after the sowing/planting date. The annual cropland produces an herbaceous cover and is sometimes combined with some tree or woody vegetation.	**Shrubland:** Geographic areas dominated by natural woody perennial plants (10% or more coverage) that lack a defined main stem and are less than 5m tall. May include scattered trees (if less than 10% coverage) and herbaceous plants at any density, with either evergreen or deciduous foliage. **Grassland:** Includes any geographic area dominated by natural herbaceous plants (plants without persistent stem or shoots above ground and lacking definite firm structure): (grasslands, prairies, steppes, savannahs, pastures) with a cover of 10% or more, irrespective of different human and/or animal activities, such as: grazing, selective fire management, etc. Woody plants (trees and/or shrubs) can be present assuming their cover is less than	10m x10m	2020 and 2021	(Zanaga et al., 2021, 2022)

		10%. It may also contain uncultivated cropland areas (without harvest/bare soil period) in the reference year.			
Dynamic world (DW)	Human planted/plotted cereals, grasses, and crops	**Shrub & Scrub:** Mix of small clusters of plants or individual plants dispersed on a landscape that shows exposed soil and rock. And scrub-filled clearings within dense forests that are clearly not taller than trees. Appear grayer/browner due to less dense leaf cover. **Grasslands:** Open areas covered in homogeneous grasses with little to no taller vegetation. This includes other homogeneous areas of grass-like vegetation (blade-type leaves) that appear distinct from trees and shrubland. The class encompasses wild cereals and grasses with no obvious human plotting (i.e., not a structured field).	10m x 10m	2–5 Days	(Brown et al., 2022)
Global Pasture Watch (GPW)	Not included in the map classification	Areas where grasses and other forage plants have been intentionally planted and managed, as well as areas of native grassland-type vegetation that clearly exhibit active and intensive management for specific human-directed uses, such as directed grazing of livestock	30m x 30m	Annual from 2000 to 2022	(Parente et al., 2024)

228

https://doi.org/10.5194/egusphere-2026-3696
Preprint. Discussion started: 2 July 2026

2.4- Agroforestry extent estimation in Europe and the Sahel

We quantified agroforestry extent as the fraction of tree canopy cover within agricultural lands, providing a spatially explicit and continuous measure. This approach captures agroforestry as a structural gradient, ranging from low-density systems (1–10% canopy cover) to high-density configurations (>51%).

We first generated a binary tree canopy map at 1m spatial resolution (tree canopy = 1, other = 0), which was then aggregated to a 30 m × 30 m grid. This resolution was chosen to be small enough to represent well the heterogeneity of agroforestry systems and ensure computational feasibility at large scales. For each 30m cell, fractional canopy cover was calculated by summing tree pixels and normalizing by the total cell area, yielding a continuous raster of percentage cover (0–100%). The aggregation was performed over a sinusoidal equal-area projection grid to ensure that all pixels have the same area ($\simeq 900m^2$) to allow for valid comparisons across regions.

Agroforestry extent was then quantified by summing the area of agricultural pixels within canopy classes, and converting pixel area to hectares ($1\ m^2 = 10^{-4}$ ha). All spatial data processing and area calculations were performed in Google Earth Engine (Gorelick et al., 2017) using the Python API. Map rendering was performed using the Geemap package (Wu, 2020) and QGIS.

https://doi.org/10.5194/egusphere-2026-3696
Preprint. Discussion started: 2 July 2026

3 Results

3.1- Agroforestry trees maps accuracy

3.1.1 - Global accuracy

Global LULC products show marked differences in performance in detecting agroforestry trees. Figure 2 summarizes the classification performance of the ESRI, ESA, and DW products, evaluated both individually (with HFI filter) and in combination with the GPW pasture mask.

Among the standalone products, the ESRI-based map achieved the highest producer's accuracy (77.2%), substantially outperforming ESA (69%) and DW (68%) products.

Combining cropland masks with the GPW pasture layer substantially reduced sensitivity (agroforestry detection) across all products. The reduction is most pronounced for ESA × GPW (32%), suggesting that the GPW pasture delineation excludes many areas containing agroforestry systems, particularly when combined with ESA and DW cropland masks. In contrast, the ESRI × GPW combination demonstrated higher sensitivity (48%), indicating that the ESRI-based cropland mask includes more agroforestry trees than other LULC products. These discrepancies highlight fundamental differences in how agricultural lands are delineated across these LULC products.

All products demonstrated high specificity for non-agroforestry tree-cover, ranging from 94.0% (ESRI) to 99.4% (ESA × GPW). While GPW intersections maximized exclusion of non-agroforestry trees, they did so at the cost of substantial omission errors for identifying agroforestry. Overall, the standalone ESRI-based agroforestry map provides the optimal trade-off: it captures a high proportion of agroforestry trees (77%) while excluding most non-agroforestry tree cover (94%).

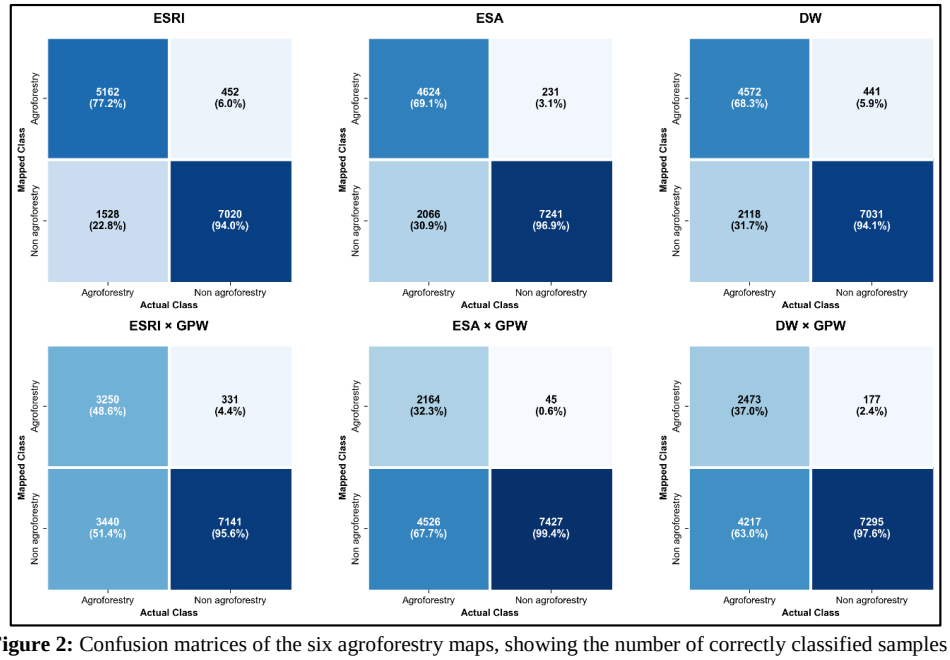

Figure 2: Confusion matrices of the six agroforestry maps, showing the number of correctly classified samples (diagonal cells) and misclassified samples (off-diagonal cells) (in percentage).

https://doi.org/10.5194/egusphere-2026-3696
Preprint. Discussion started: 2 July 2026

3.1.2- Classification errors across different tree-based systems

Classification performance varied markedly across tree-based system types (Fig. 3), revealing strong differences in sensitivity depending on the agroforestry system. The standalone ESRI-based agroforestry maps exhibited the most performing detection across categories, with producer accuracy of 63.6% for alley cropping, 72.8% for Scattered Agroforestry systems, and 87.8% for Hedgerows, respectively.

For non-agroforestry classes, all maps effectively exclude unmanaged trees outside forests (TOF). In contrast, woody monocrops remained difficult to distinguish from agroforestry across all datasets. The standalone ESRI-based map displayed the highest commission errors in this category, misclassifying 67.8% of woody monocrops as agroforestry. Other datasets demonstrated superior exclusion of woody monocrops, with values ranging from 37% for the DW-based map down to 19% for the ESA x GPW-based map. However, these lower values rather result from a systematic omission of tree-bearing agricultural landscapes in these products.

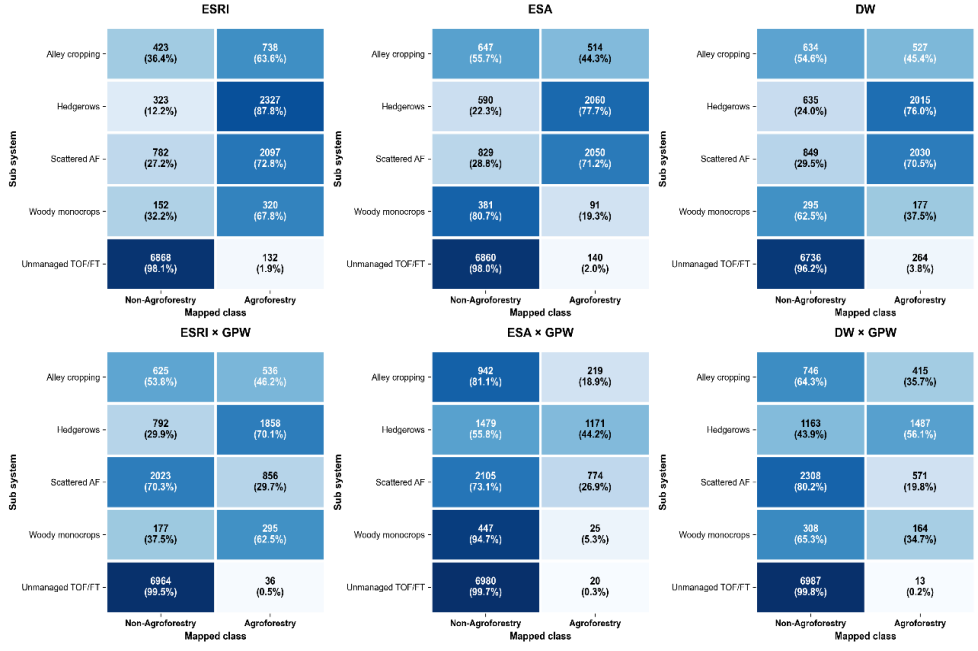

Figure 3: Confusion matrices of the agroforestry maps, each corresponding to a specific agroforestry map, showing the number as a percentage of sub-classes (alley cropping, hedgerows, scattered agroforestry, woody monocrops, and unmanaged TOF / FT) classified into the categories agroforestry trees and non-agroforestry trees

3.1.3- Accuracy per biome

Biome-level evaluation (Fig. 4) reveals that the standalone ESRI-based map consistently outperformed all other datasets across ecological zones. It achieved its highest F1 score in Temperate Grasslands/Savannas (0.93) and Tropical & Subtropical Dry Broadleaf Forests (0.89). Performance declines across all products in Mediterranean Forests and Deserts/Xeric Shrublands, reflecting the greater difficulty of detecting agroforestry in arid and semi-arid systems. Even in these challenging biomes, the ESRI-based map maintains relatively high (F1= 0.79). The

https://doi.org/10.5194/egusphere-2026-3696
Preprint. Discussion started: 2 July 2026

ability of the ESRI-based map to maintain high detection rates across diverse environments demonstrates its robustness and supports its use for large-scale agroforestry extent estimation across contrasting environmental contexts.

Figure 4: F1-score of the six agroforestry maps across different biomes

3.2- Agroforestry extent in Europe and the Sahel

Using the ESRI-based agroforestry map (Fig 5), we estimate that 86 Mha in Europe and 36 Mha in the Sahel (Table 2) of agricultural lands are under agroforestry, representing 9% and 10.8% of the total area of these regions, respectively. Agroforestry systems in Europe occur predominantly on croplands, covering 47 Mha (Figure 5), while pastures with trees occupy 38 Mha. In the Sahel, pasture lands with trees dominate the agroforestry

https://doi.org/10.5194/egusphere-2026-3696
Preprint. Discussion started: 2 July 2026

landscape, covering 35 Mha and representing 97% of the total agroforestry extent in the region, whereas croplands with trees account for only 1.17 Mha.

Temperate Broadleaf & Mixed Forests biome accounts for the largest share of agricultural lands with tree cover in Europe, with 49 Mha representing 11 % of the total biome area (Table 2) , followed by the Mediterranean Forests/Woodlands/Scrub biome (Southern Europe) with 20 Mha, and the highest agroforestry coverage rate among all biomes, with 21% of its total area under agroforestry. Northern biomes contribute comparatively little, with 6.2 Mha in boreal and 0.61 Mha in tundra regions

The Sahel region is overwhelmingly dominated by the Tropical & Subtropical Grasslands/Savannas biome (93% of Sahel total area) with 33.9 Mha of treed agricultural lands representing 10.8 % of the biome area. Other biomes each contribute less than 3 Mha of agroforestry extent.

Tree canopy cover within agroforestry systems spans a broad continuum, reflecting the structural diversity of these land use systems. Across both regions, agroforestry extent decreases with increasing canopy cover, following a decay-like distribution (Fig 5.D). Open-canopy systems (1–10% tree cover) dominate in both regions, accounting for 32 Mha (37%) in Europe and 21.4 Mha (59%) in the Sahel (Table 2). Intermediate canopy cover systems (10–50%) represent a substantial share of agroforestry extent, covering 38.6 Mha in Europe and 13.3 Mha in the Sahel. In contrast, dense canopy systems (> 50% tree cover) are relatively rare, occupying 15.2 Mha in Europe and less than 1.7 Mha in the Sahel.

https://doi.org/10.5194/egusphere-2026-3696
Preprint. Discussion started: 2 July 2026

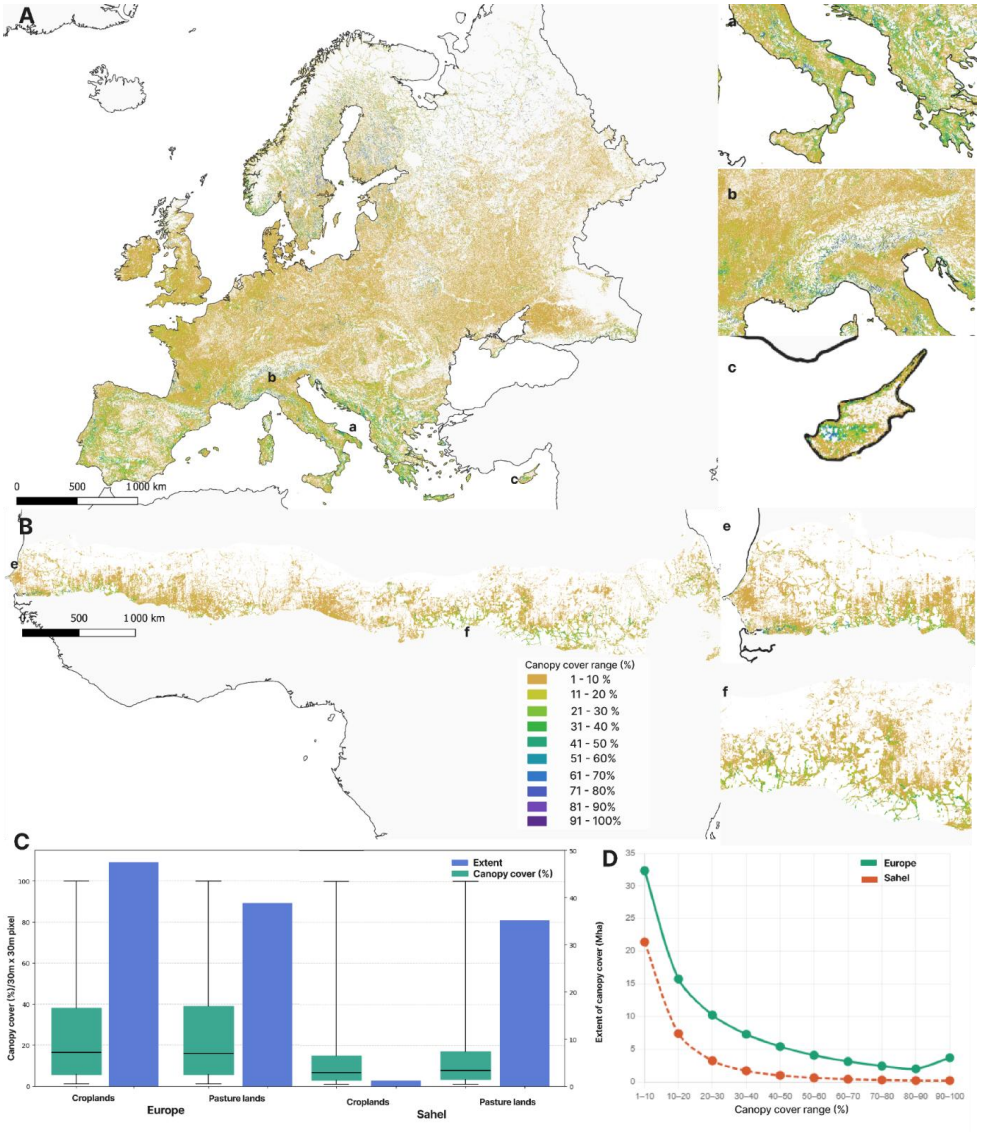

Figure 5: Spatial distribution of tree canopy cover (%) on agricultural lands in Europe (A) and the Sahel (B), aggregated to 1 km × 1 km resolution for visualisation (original resolution: 30 m × 30 m; a pixel with 10% canopy cover corresponds to 90 m² of tree cover). (C) Distribution of tree canopy cover per land use class (pixels with ≥ 1% canopy cover), where boxes represent Q1 (25th percentile), median, and Q3 (75th percentile) estimated using histogram-based quantile estimation, and bars indicate the total extent (Mha) of each land use class with at least 1% canopy cover. (D) Agroforestry extent (Mha) per tree canopy cover range in Europe and the Sahel. Coastline basemap was derived from Natural Earth (https://www.naturalearthdata.com).

Table 2: Areal extent of agricultural land with at least 1% tree canopy cover in Europe and the Sahel region, in million hectares (Mha). These estimates are obtained by aggregating to 30 m × 30 m spatial resolution the 1m spatial-resolution ESRI-based agroforestry tree canopy map. The biome area is calculated per region, not the full biome area, using the geodesic method

Region	Tree cover range (%) / WWF biomes	1-10	10-20	20-30	30-40	40-50	50-60	60-70	70-80	80-90	> 90	Total (Mha)	Biome area (Mha)	Biome area (%)
Europe	Temperate Broadleaf & Mixed Forests	18.73	9.08	5.90	4.19	3.04	2.24	1.67	1.28	1.03	1.95	49.10	443.87	11.06
	Mediterranean Forests, Woodlands & Scrub	7.37	3.89	2.54	1.78	1.31	0.98	0.76	0.59	0.48	0.66	20.36	93.30	21.82
	Temperate Grasslands, Savannas & Shrublands	2.55	1.19	0.81	0.64	0.53	0.44	0.35	0.27	0.21	0.28	7.28	97.45	7.47
	Boreal Forests / Taiga	2.46	1.01	0.61	0.43	0.32	0.25	0.20	0.18	0.17	0.59	6.22	227.01	2.74
	Temperate Conifer Forests	0.93	0.44	0.27	0.19	0.14	0.11	0.09	0.07	0.06	0.16	2.48	31.27	7.93
	Tundra	0.25	0.11	0.07	0.05	0.03	0.03	0.02	0.02	0.02	0.03	0.61	51.26	1.20
	Deserts & Xeric Shrublands	0.06	0.02	0.01	0.01	0.01	0.004	0.003	0.002	0.002	0.002	0.12	8.69	1.39
	Total	**32.34**	**15.74**	**10.21**	**7.28**	**5.38**	**4.06**	**3.10**	**2.41**	**1.97**	**3.67**	**86.17**	**952.85**	**9.04**
Sahel	Tropical & Subtropical Grasslands, Savannas & Shrublands	20.14	6.90	2.98	1.53	0.88	0.55	0.36	0.24	0.16	0.15	33.90	313.77	10.80
	Flooded Grasslands & Savannas	0.52	0.20	0.10	0.05	0.03	0.02	0.01	0.01	0.01	0.01	0.97	11.49	8.41
	Tropical & Subtropical Moist Broadleaf Forests	0.41	0.16	0.08	0.05	0.03	0.02	0.01	0.01	0.01	0.01	0.79	4.59	17.21
	Montane Grasslands & Shrublands	0.25	0.09	0.05	0.03	0.02	0.01	0.01	0.01	0.00	0.01	0.46	3.15	14.77
	Deserts & Xeric Shrublands	0.09	0.03	0.01	0.01	0.004	0.002	0.002	0.001	0.001	0.001	0.15	2.55	5.99
	Mangroves	0.0046	0.0021	0.0011	0.0006	0.0004	0.0002	0.0002	0.0001	0.0001	0.0001	0.01	0.15	6.21
	Total	**21.072**	**7.541**	**3.297**	**1.715**	**0.994**	**0.620**	**0.407**	**0.276**	**0.192**	**0.188**	**36.30**	**335.70**	**10.81**

https://doi.org/10.5194/egusphere-2026-3696
Preprint. Discussion started: 2 July 2026

4 - Discussion

In this analysis, we investigated the potential of integrating high-resolution Land Use and Land Cover (LULC) products (ESRI, ESA, DW, and GPW) with a very high-resolution (1m) tree canopy map to detect agroforestry at the individual tree level. This approach represents a shift away from traditional coarse-resolution tree cover datasets (e.g., Hansen et al. (2013)), and enables a more explicit evaluation of inclusion and exclusion errors across agroforestry systems and non-agroforestry land uses.

The primary objective was to assess whether this high-resolution integration can address persistent mapping limitations in large-scale agroforestry mapping. Specifically, we evaluate: (1) the ability of high-resolution LULC data to limit the mixed-pixel effects; (2) whether 1m canopy data improve the detection of individual scattered trees within agricultural landscapes; and (3) how adopting an inclusive definition of agroforestry influences extent estimates. Together, these components aim to reduce systematic omission of both dense and low-density agroforestry systems, providing a more realistic representation of agroforestry in the landscape.

4.1- Overlaying land use and land cover data

Despite relying on similar Sentinel-2 satellite imagery inputs and comparable spatial and temporal resolutions, the evaluated LULC products showed substantial differences in performance when overlaid with the same tree canopy cover map and validated against the same reference data. The standalone ESRI based map consistently outperformed alternative global datasets, indicating that the definition of the agricultural mask is a critical driver of agroforestry detection. This finding presents a semantic paradox: ESRI's official definition describes cropland as vegetation 'not at tree height,' a constraint that should theoretically exclude agroforestry. However, our analysis reveals that pixels containing agroforestry trees are frequently retained within the 'Cropland' or 'Rangeland' classes, rather than being assigned to 'Tree Cover.'

We hypothesize that this behavior stems from training data that likely included mixed tree-crop landscapes labeled by annotators as 'croplands' when training the ESRI's classification model, causing the model to learn and replicate this interpretation. Consequently, ESRI maintains a spatially contiguous agricultural mask, whereas other products tend to fragment agroforestry systems by isolating canopy elements as 'Tree cover'. While this generalization limits the ability of ESRI to distinguish monocrops from agroforestry, it provides the optimal base layer for our methodology. Overlaying the high-resolution (1m) tree canopy map onto this broad agricultural mask effectively resolves the limitation, combining ESRI's broad functional identification of cropland with the precise structural detection of trees to accurately map agroforestry trees. This result highlights that agroforestry estimates are highly sensitive to the choice of LULC product. Previous studies may therefore substantially under or over-estimate tree cover on agricultural lands due to uncertainties in land use and land cover classification. For instance, (Liu et al., 2023) report only 2.67 Mha of tree-covered agricultural land in Europe, which is far smaller than our 86 Mha estimates. Visual inspection suggests that this discrepancy is partly due to misclassification of linear features such as hedgerows, a dominant agroforestry system in Europe (Rubio-Delgado et al., 2024) , as built-up areas in Hansen et al. (2022)-based products.

Visual investigation comparing the agroforestry map to baseline satellite data further revealed that our approach also captures trees at forest edges and within small forest patches embedded in agricultural lands, consistent with our operational agroforestry definition. The inclusion of such trees remains debated in the literature (Golicz et al.,

https://doi.org/10.5194/egusphere-2026-3696
Preprint. Discussion started: 2 July 2026

2022; Terasaki Hart et al., 2023), as they may not be intentionally managed within the same land use unit. However, excluding such systems risks overlooking important ecosystem services that are provided by trees adjacent to cropland and pasture land. For instance, alley cropping (integrated with cropland) may provide provisioning services such as fruit or timber, while forest patch edges (which may not be managed together with adjacent croplands) may be efficient in delivering regulating and cultural services, such as habitat provision and recreation. Restricting the definition to systems in the same management unit would therefore lead to an incomplete representation of the ecosystem services delivered by trees on agricultural land. We thus adopt an inclusive function-based definition that encompasses all trees exerting an influence on agricultural land, regardless of the intentionality of their establishment and the integration of their management.

Our validation indicated that 68% of samples labeled as woody monocrops were misclassified as agroforestry by our mapping approach, highlighting a significant limitation of the simple overlay approach. Importantly, this limitation is not specific to our approach but reflects a more general challenge in large-scale agroforestry mapping. Distinguishing agroforestry from woody monocrops requires information on spatial structure, planting patterns, or management practices, which cannot be captured by LULC data alone. Addressing this ambiguity would therefore require more advanced classification approaches, such as machine learning or deep learning models trained on very high-resolution imagery, potentially combined with additional data sources (e.g., SAR or temporal dynamics).

Finally, our map is constrained by its restriction to the agroforestry systems occurring on agricultural land uses, which leads to the exclusion of 'agroforests' or complex systems occurring within forest land cover classes. This binary definition risks underestimating closed-canopy systems (e.g., shaded perennial systems). To address these limitations, recent work by the FAO suggests adopting a 'likelihood map' approach (FAO, 2025), in forested regions where detecting closed-canopy agroforestry systems using optical satellite imagery is challenging.

https://doi.org/10.5194/egusphere-2026-3696
Preprint. Discussion started: 2 July 2026

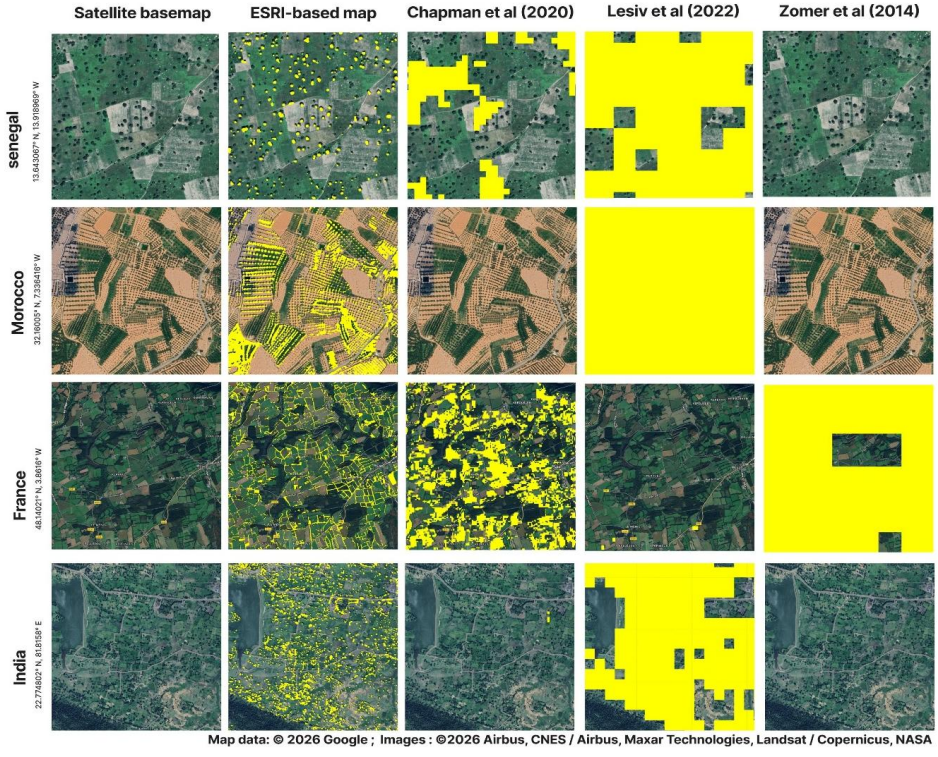

Figure 6: Comparative visualization of agroforestry detection across four study regions: Senegal, Morocco, France, and India. The ESRI-based map (current study) identifies individual agroforestry trees (yellow) at a 1 m x 1 m resolution. For comparison, the native spatial resolutions of global datasets are indicated: Chapman et al. (2020) at 30m x 30m, Lesiv et al. (2022) at 100m x 100m, and Zomer et al. (2014) at 1km x 1km. Map data: © 2026 Google; Images: ©2026 Airbus, CNES / Airbus, Maxar Technologies, Landsat / Copernicus, NASA

While the 1m tree canopy map substantially improved the detection of scattered agroforestry trees compared to existing baselines (Fig. 6), it failed to detect approximately 36% of alley cropping samples. We attribute this limitation to the spatiotemporal trade-offs inherent in remote sensing: High-resolution sensors typically have lower revisit frequencies than coarser-resolution platforms (Justice et al., 2002), creating blind spots that limit the detection of dynamic agroforestry systems. Two main factors likely contribute to this limitation at annual temporal resolutions. First, agroforestry systems are highly dynamic, with rapid structural change due to economic, agronomic, institutional, and demographic factors (Escobar-Ocampo et al., 2023). For instance, farmers may actively reduce tree cover (e.g., pruning to manage pests or regulate shade), or favor deciduous species to limit competition for light (Piotto et al., 2024). However, such management choices can render trees temporarily undetectable, particularly if imagery is acquired during leaf-off periods. Second, atmospheric constraints further exacerbate detection bias: the scarcity of cloud-free observations often necessitates the use of image composites biased toward the dry season; this reliance on dry-season data, when trees may be leafless or

https://doi.org/10.5194/egusphere-2026-3696
Preprint. Discussion started: 2 July 2026

stressed, can lead to a systematic underestimation of tree cover in sub-humid and dry regions (Brandt et al., 2023).

4.2- Agroforestry extent estimation.

Our regional estimates differ substantially from previous global and regional assessments (Fig. 7). These discrepancies are primarily attributable to differences in methodological choices, spatial resolution, and the operational definition of agroforestry adopted across studies. For instance, Chapman et al. (2020) analyse the extent of agricultural lands with woody biomass, which we interpret as a proxy for agroforestry systems, defined by tree cover lower than 25% and above-ground carbon biomass exceeding 5 MgC/ha. This restrictive definition excludes agroforestry systems where tree cover surpasses the 25% threshold (Terasaki Hart et al., 2023). More critically, the biomass threshold leads to a systematic underestimation in low-biomass systems, particularly in drylands. This constraint likely explains why Chapman's estimate only 7.21 Mha of agroforestry in the Sahel—an underestimation of ~80% compared to our estimate of 36.3 Mha.

Similarly, spatial resolution plays a pivotal role in the discrepancy observed with Zomer et al. (2014), who defined agroforestry as 1km agricultural pixels with tree cover greater than 10%. This threshold excludes low-density systems, particularly in regions characterized by scattered trees. As a result, Zomer et al. (2009) estimate 7.86 Mha of agroforestry in the Sahel, corresponding to an underestimation of 78.3% compared to our results. Conversely, coarse-resolution data are prone to overestimating extent in fragmented landscapes where forests and agricultural lands co-occur within the same pixel. In Europe, this "mixed pixel" effect resulted in an overestimation of 186% (246 Mha) compared to our estimate of 86 Mha; this overestimation of agroforestry in European landscapes by Zomer et al. (2009) was reported by Den Herder et al. (2017).

Discrepancies also arise from the limitations inherent to machine learning approaches based on optical satellite data, as illustrated in Lesiv et al. (2022). Their study recognized frequent spectral confusion between agroforestry and naturally regenerating managed forests, resulting in a 21% underestimation (67 Mha) in Europe compared to our 86 Mha. This issue may also stem from errors introduced during the training data generation phase, particularly in photo-interpretation, where "sparse trees on agricultural land" are often misclassified as "sparse natural forest," especially in temperate regions. Recent work by Tahiri et al. (2026) addresses this limitation by providing a classification method based on the photo-interpretation of very high-resolution satellite data. Adopting this approach could improve sampling details and provide clearer training samples for machine learning algorithms. Furthermore, combining such data with Synthetic Aperture Radar (SAR) data, which provide complementary structural information, could help reduce spectral confusion and improve classification performance.

In the European Union, alternative approaches based on the LUCAS (Land Use/Cover Area frame Survey) dataset (Den Herder et al., 2017; Rubio-Delgado et al., 2023) estimated agroforestry extent from the spatial distribution of labeled points per country. While LUCAS integrates photo-interpretation and field observations, providing detailed information on crop and tree types, it presents notable limitations for large-scale, spatially explicit estimation. In particular, its applicability is restricted to Europe, and its coarse sampling grid (2 km) implies a low probability of intersecting individual trees, which are often sparsely distributed in agricultural

https://doi.org/10.5194/egusphere-2026-3696
Preprint. Discussion started: 2 July 2026

landscapes. As a result, this approach likely underestimates the extent of agroforestry and, more broadly, trees on farmland.

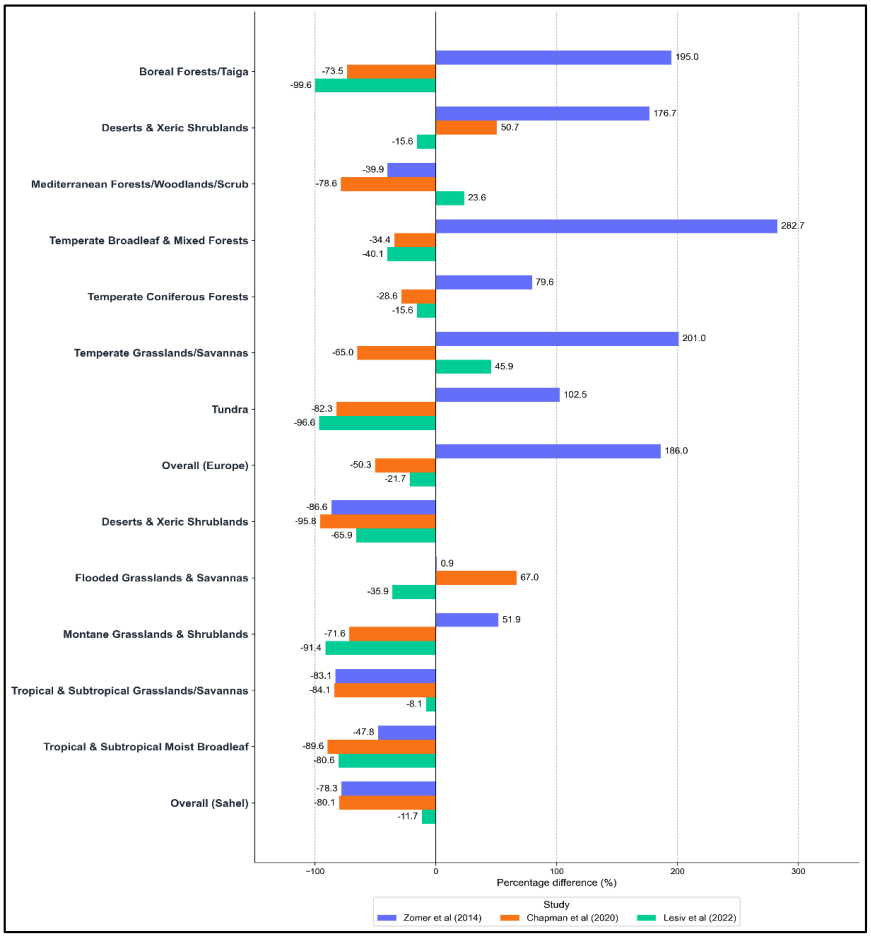

Figure 7: Relative difference (%) between the new map (ESRI-based map) and previous large-scale agroforestry mapping studies (Chapman et al., 2020; Lesiv et al., 2022; Zomer et al., 2009), aggregated by biome and region. The relative difference is calculated as: (Previous study estimates - our estimates) / our estimates x 100. The area was estimated for each author using the data they provided and their definition of agroforestry.

4.3- Minimum mapping unit of agroforestry

Delineating a functional agroforestry unit remains a critical challenge in mapping efforts, as agroforestry is a continuum of interactions between trees and the agricultural matrix. While most prior attempts implicitly equate the agroforestry unit with a fixed minimum mapping unit (i.e., the pixel) as a compromise between resolution and computational constraints, our analysis adopts a distinct approach by starting from individual tree canopy delineations and reconstructing the agroforestry unit outward from their spatial context within the agricultural matrix. This contrasts with medium-resolution datasets such as (Hansen et al., 2013), where each pixel

https://doi.org/10.5194/egusphere-2026-3696
Preprint. Discussion started: 2 July 2026

represents a prediction of tree cover percentage without the ability to distinguish individual trees. Furthermore, individual agroforestry tree detection offers the flexibility to define the "agroforestry unit" dynamically. This flexibility is essential because the spatial extent of tree influence is not static; it varies with tree species, ecosystem service, pedoclimatic context, and agricultural practices (Baker et al., 2025; Laura et al., 2017; Sileshi, 2016). For instance, trees can influence soil organic carbon stocks up to 30 m from the trunk (Laura et al., 2017), crop yield up to 17 m (Roupsard et al., 2020), and soil biota up to 18 m (Vaupel et al., 2023). By detecting individual trees, we avoid the bias introduced by fixing the size of an agroforestry unit a priori to a pixel size, allowing for a more flexible treatment of spatial variability and context-specific interactions.

5- Conclusion

Agroforestry has been the subject of numerous large-scale mapping studies. However, existing maps are constrained by fundamental limitations stemming from data resolution, which generate two critical issues: (i) over-estimation of agroforestry extent due to the inclusion of non-agroforestry trees and (ii) systematic underestimation of tree cover in heterogeneous agricultural landscapes. This study addresses these limitations through two methodological advances: the application of high-resolution land use and land cover (LULC) data and the integration of individual tree canopy maps to enable tree-level representation. Our analysis reveals that even when different LULC products share identical spatial resolution (10m), their sensitivity and specificity errors diverge substantially, indicating that classification definitions and training methodologies used to generate LUCL datasets significantly influence agroforestry detection. Based on a validation against 14,162 georeferenced ground-truth observations distinguishing agroforestry from non-agroforestry trees, an ESRI-based land-use mask was identified as the most reliable land-use product (accuracy: 77.2%). Furthermore, we demonstrate that simple LUCL-tree overlay approaches, while improved by higher resolution data, remain susceptible to misclassification errors, particularly the misidentification of woody monoculture crops as agroforestry systems. These findings suggest two pathways forward: first, the adoption of more sophisticated analytical frameworks, including machine learning models capable of distinguishing complex land use patterns; and second, a shift toward likelihood-based agroforestry maps that accommodate the gradient of tree-agriculture-forest integration, rather than relying on strict, binary classification schemes.

6- Code and data availability

The code used in this study is available at: https://github.com/ouadyatahiri/Agroforestry-mapping (last access: 21 June; https://doi.org/10.5281/zenodo.20782941, Tahiri 2026). Resulting maps are available at: https://doi.org/10.5281/zenodo.20257798 . Dataset used for validation is available at : https://doi.org/10.5281/zenodo.20261860

7- Author contributions

All authors contributed to conceptualisation and study design, data validation, interpretation of results, manuscript drafting, and critical revision. Ouadya TAHIRI additionally contributed to data acquisition, processing, and analysis.

8- Competing interests

The corresponding author has declared that none of the authors has any competing interests.

9- Acknowledgements

https://doi.org/10.5194/egusphere-2026-3696
Preprint. Discussion started: 2 July 2026

During the preparation of this work, the author(s) used Claude and Google GEMINI in order to assist in drafting, paraphrasing, and language editing of the manuscript. After using this tool/service, the author(s) reviewed and edited the content as needed and take(s) full responsibility for the content of the published article.

No generative AI or AI-assisted tools were used to create, alter, or manipulate any images presented in this manuscript. All figures and images are original and accurately represent the data.

10- Financial support

This work benefited from the French state aid managed by the ANR under the "Investissements d'avenir" programme with the reference ANR-16-CONV-0003 as a partial stipend, alongside a partial stipend from CIRAD (Centre de coopération Internationale en Recherche Agronomique pour le Développement). The funding sources had no role in the study design, data collection, analysis, or decision to publish.

11- References

Baker, T. P., England, J. R., Brooks, S. T., Stewart, S. B., and Mendham, D.: Effect of silvopasture, paddock trees and linear agroforestry systems on agricultural productivity: A global quantitative analysis, Agric. Syst., 224, 104240, https://doi.org/10.1016/j.agsy.2024.104240, 2025.

Beillouin, D., Ben-Ari, T., Malézieux, E., Seufert, V., and Makowski, D.: Positive but variable effects of crop diversification on biodiversity and ecosystem services, Glob. Change Biol., 27, 4697–4710, https://doi.org/10.1111/gcb.15747, 2021.

Bolívar-Santamaría, S. and Reu, B.: Detection and characterization of agroforestry systems in the Colombian Andes using sentinel-2 imagery, Agrofor. Syst., 95, 499–514, https://doi.org/10.1007/s10457-021-00597-8, 2021.

Brandt, J., Ertel, J., Spore, J., and Stolle, F.: Wall-to-wall mapping of tree extent in the tropics with Sentinel-1 and Sentinel-2, Remote Sens. Environ., 292, 113574, https://doi.org/10.1016/j.rse.2023.113574, 2023.

Brandt, M., Tucker, C. J., Kariryaa, A., Rasmussen, K., Abel, C., Small, J., Chave, J., Rasmussen, L. V., Hiernaux, P., Diouf, A. A., Kergoat, L., Mertz, O., Igel, C., Gieseke, F., Schöning, J., Li, S., Melocik, K., Meyer, J., Sinno, S., Romero, E., Glennie, E., Montagu, A., Dendoncker, M., and Fensholt, R.: An unexpectedly large count of trees in the West African Sahara and Sahel, Nature, 587, 78–82, https://doi.org/10.1038/s41586-020-2824-5, 2020.

Brown, C. F., Brumby, S. P., Guzder-Williams, B., Birch, T., Hyde, S. B., Mazzariello, J., Czerwinski, W., Pasquarella, V. J., Haertel, R., Ilyushchenko, S., Schwehr, K., Weisse, M., Stolle, F., Hanson, C., Guinan, O., Moore, R., and Tait, A. M.: Dynamic World, Near real-time global 10 m land use land cover mapping, Sci. Data, 9, 251, https://doi.org/10.1038/s41597-022-01307-4, 2022.

Cardinael, R., Umulisa, V., Toudert, A., Olivier, A., Bockel, L., and Bernoux, M.: Revisiting IPCC Tier 1 coefficients for soil organic and biomass carbon storage in agroforestry systems, Environ. Res. Lett., 13, 124020, https://doi.org/10.1088/1748-9326/aaeb5f, 2018.

Chapman, M., Walker, W. S., Cook-Patton, S. C., Ellis, P. W., Farina, M., Griscom, B. W., and Baccini, A.: Large climate mitigation potential from adding trees to agricultural lands, Glob. Change Biol., 26, 4357–4365, https://doi.org/10.1111/gcb.15121, 2020.

https://doi.org/10.5194/egusphere-2026-3696
Preprint. Discussion started: 2 July 2026

584 Christen, P., Hand, D. J., and Kirielle, N.: A Review of the F-Measure: Its History, Properties,
585 Criticism, and Alternatives, ACM Comput. Surv., 56, 1–24, https://doi.org/10.1145/3606367,
586 2024.

587 Den Herder, M., Moreno, G., Mosquera-Losada, R. M., Palma, J. H. N., Sidiropoulou, A.,
588 Santiago Freijanes, J. J., Crous-Duran, J., Paulo, J. A., Tomé, M., Pantera, A.,
589 Papanastasis, V. P., Mantzanas, K., Pachana, P., Papadopoulos, A., Plieninger, T., and
590 Burgess, P. J.: Current extent and stratification of agroforestry in the European Union, Agric.
591 Ecosyst. Environ., 241, 121–132, https://doi.org/10.1016/j.agee.2017.03.005, 2017.

592 Diouf, A. A.: Mapping present and future agroforestry in Africa, Center for Development
593 Research (ZEF), University of Bonn, https://hdl.handle.net/10419/315037, 2025.

594 Escobar-Ocampo, M. C., Castillo-Santiago, M. Á., Ochoa-Gaona, S., Enríquez, P. L.,
595 Mondragón-Vázquez, E., Espinosa-Jiménez, F. R., and Sibelet, N.: Drivers of Land-Use
596 Change in Agroforestry Landscapes of Southern Mexico, Hum. Ecol., 51, 409–422,
597 https://doi.org/10.1007/s10745-023-00417-w, 2023.

598 FAO: Beyond the canopy: Mapping cocoa fields in Cameroon's agroforestry systems for a
599 deforestation-free cocoa, https://www.fao.org/investment-centre/latest/news/detail/beyond-
600 the-canopy--mapping-cocoa-fields-in-cameroon-s-agroforestry-systems-for-a-deforestation-
601 free-cocoa/en, 29 December 2025.

602 Gassert, F., Venter, O., Watson, J. E. M., Brumby, S. P., Mazzariello, J. C., Atkinson, S. C.,
603 and Hyde, S.: An operational approach to near real time global high resolution mapping of
604 the terrestrial Human Footprint, Front. Remote Sens., 4, 1130896,
605 https://doi.org/10.3389/frsen.2023.1130896, 2023.

606 Gorelick, N., Hancher, M., Dixon, M., Ilyushchenko, S., Thau, D., and Moore, R.: Google
607 Earth Engine: Planetary-scale geospatial analysis for everyone, Remote Sens. Environ.,
608 202, 18–27, https://doi.org/10.1016/j.rse.2017.06.031, 2017.

609 Hansen, M. C., Potapov, P. V., Moore, R., Hancher, M., Turubanova, S. A., Tyukavina, A.,
610 Thau, D., Stehman, S. V., Goetz, S. J., Loveland, T. R., Kommareddy, A., Egorov, A., Chini,
611 L., Justice, C. O., and Townshend, J. R. G.: High-Resolution Global Maps of 21st-Century
612 Forest Cover Change, Science, 342, 850–853, https://doi.org/10.1126/science.1244693,
613 2013.

614 Hansen, M. C., Potapov, P. V., Pickens, A. H., Tyukavina, A., Hernandez-Serna, A., Zalles,
615 V., Turubanova, S., Kommareddy, I., Stehman, S. V., Song, X.-P., and Kommareddy, A.:
616 Global land use extent and dispersion within natural land cover using Landsat data, Environ.
617 Res. Lett., 17, 034050, https://doi.org/10.1088/1748-9326/ac46ec, 2022.

618 IPCC: IPCC Special Report on Land Use, Land-Use Change and Forestry, Cambridge Univ.
619 Press, ISBN: 92-9169-114-3, 2000.

620 Ivezić, V., Yu, Y., and Werf, W. V. D.: Crop Yields in European Agroforestry Systems: A
621 Meta-Analysis, Front. Sustain. Food Syst., 5, 606631,
622 https://doi.org/10.3389/fsufs.2021.606631, 2021.

623 Jones, S. K., Sánchez, A. C., Juventia, S. D., and Estrada-Carmona, N.: A global database
624 of diversified farming effects on biodiversity and yield, Sci. Data, 8, 212,
625 https://doi.org/10.1038/s41597-021-01000-y, 2021.

https://doi.org/10.5194/egusphere-2026-3696
Preprint. Discussion started: 2 July 2026

626 Justice, C. O., Townshend, J. R. G., Vermote, E. F., Masuoka, E., Wolfe, R. E., Saleous, N.,
627 Roy, D. P., and Morisette, J. T.: An overview of MODIS Land data processing and product
628 status, Remote Sens. Environ., 83, 3–15, https://doi.org/10.1016/S0034-4257(02)00084-6,
629 2002.

630 Karra, K., Kontgis, C., Statman-Weil, Z., Mazzariello, J. C., Mathis, M., and Brumby, S. P.:
631 Global land use / land cover with Sentinel 2 and deep learning, in: 2021 IEEE International
632 Geoscience and Remote Sensing Symposium IGARSS, IGARSS 2021 - 2021 IEEE
633 International Geoscience and Remote Sensing Symposium, 4704–4707,
634 https://doi.org/10.1109/IGARSS47720.2021.9553499, 2021.

635 Laura, V. V., Bert, R., Steven, B., Pieter, D. F., Victoria, N., Paul, P., and Kris, V.: Ecosystem
636 service delivery of agri-environment measures: A synthesis for hedgerows and grass strips
637 on arable land, Agric. Ecosyst. Environ., 244, 32–51,
638 https://doi.org/10.1016/j.agee.2017.04.015, 2017.

639 Lesiv, M., Schepaschenko, D., Buchhorn, M., See, L., Dürauer, M., Georgieva, I., Jung, M.,
640 Hofhansl, F., Schulze, K., Bilous, A., Blyshchyk, V., Mukhortova, L., Brenes, C. L. M.,
641 Krivobokov, L., Ntie, S., Tsogt, K., Pietsch, S. A., Tikhonova, E., Kim, M., Di Fulvio, F., Su,
642 Y.-F., Zadorozhniuk, R., Sirbu, F. S., Panging, K., Bilous, S., Kovalevskii, S. B., Kraxner, F.,
643 Rabia, A. H., Vasylyshyn, R., Ahmed, R., Diachuk, P., Kovalevskyi, S. S., Bungnamei, K.,
644 Bordoloi, K., Churilov, A., Vasylyshyn, O., Sahariah, D., Tertyshnyi, A. P., Saikia, A., Malek,
645 Ž., Singha, K., Feshchenko, R., Prestele, R., Akhtar, I. U. H., Sharma, K., Domashovets, G.,
646 Spawn-Lee, S. A., Blyshchyk, O., Slyva, O., Ilkiv, M., Melnyk, O., Sliusarchuk, V., Karpuk,
647 A., Terentiev, A., Bilous, V., Blyshchyk, K., Bilous, M., Bogovyk, N., Blyshchyk, I., Bartalev,
648 S., Yatskov, M., Smets, B., Visconti, P., Mccallum, I., Obersteiner, M., and Fritz, S.: Global
649 forest management data for 2015 at a 100 m resolution, Sci. Data, 9, 199,
650 https://doi.org/10.1038/s41597-022-01332-3, 2022.

651 Liu, S., Brandt, M., Nord-Larsen, T., Chave, J., Reiner, F., Lang, N., Tong, X., Ciais, P., Igel,
652 C., Pascual, A., Guerra-Hernandez, J., Li, S., Mugabowindekwe, M., Saatchi, S., Yue, Y.,
653 Chen, Z., and Fensholt, R.: The overlooked contribution of trees outside forests to tree cover
654 and woody biomass across Europe, Sci. Adv., https://doi.org/10.1126/sciadv.adh4097, 2023.

655 Mugabowindekwe, M., Brandt, M., Chave, J., Reiner, F., Skole, D. L., Kariryaa, A., Igel, C.,
656 Hiernaux, P., Ciais, P., Mertz, O., Tong, X., Li, S., Rwanyiziri, G., Dushimiyimana, T., Ndoli,
657 A., Uwizeyimana, V., Lillesø, J.-P. B., Gieseke, F., Tucker, C. J., Saatchi, S., and Fensholt,
658 R.: Nation-wide mapping of tree-level aboveground carbon stocks in Rwanda, Nat. Clim.
659 Change, 13, 91–97, https://doi.org/10.1038/s41558-022-01544-w, 2023.

660 Nair, P. K. R.: An introduction to agroforestry, Kluwer Acad. Publ, Dordrecht, 499 pp., 1993.

661 Nair, P. K. R.: Carbon sequestration studies in agroforestry systems: a reality-check,
662 Agrofor. Syst., 86, 243–253, https://doi.org/10.1007/s10457-011-9434-z, 2012.

663 Olson, D. M., Dinerstein, E., Wikramanayake, E. D., Burgess, N. D., Powell, G. V. N.,
664 Underwood, E. C., D'amico, J. A., Itoua, I., Strand, H. E., Morrison, J. C., Loucks, C. J.,
665 Allnutt, T. F., Ricketts, T. H., Kura, Y., Lamoreux, J. F., Wettengel, W. W., Hedao, P., and
666 Kassem, K. R.: Terrestrial Ecoregions of the World: A New Map of Life on Earth, BioScience,
667 51, 933, https://doi.org/10.1641/0006-3568(2001)051%5B0933:TEOTWA%5D2.0.CO;2,
668 2001.

669 Parente, L., Sloat, L., Mesquita, V., Consoli, D., Stanimirova, R., Hengl, T., Bonannella, C.,
670 Teles, N., Wheeler, I., Hunter, M., Ehrmann, S., Ferreira, L., Mattos, A. P., Oliveira, B.,
671 Meyer, C., Şahin, M., Witjes, M., Fritz, S., Malek, Z., and Stolle, F.: Annual 30-m maps of

https://doi.org/10.5194/egusphere-2026-3696
Preprint. Discussion started: 2 July 2026

global grassland class and extent (2000–2022) based on spatiotemporal Machine Learning, Sci. Data, 11, 1303, https://doi.org/10.1038/s41597-024-04139-6, 2024.

Reiner, F., Brandt, M., Tong, X., Skole, D., Kariryaa, A., Ciais, P., Davies, A., Hiernaux, P., Chave, J., Mugabowindekwe, M., Igel, C., Oehmcke, S., Gieseke, F., Li, S., Liu, S., Saatchi, S., Boucher, P., Singh, J., Taugourdeau, S., Dendoncker, M., Song, X.-P., Mertz, O., Tucker, C. J., and Fensholt, R.: More than one quarter of Africa's tree cover is found outside areas previously classified as forest, Nat. Commun., 14, 2258, https://doi.org/10.1038/s41467-023-37880-4, 2023.

Roupsard, O., Audebert, A., Ndour, A. P., Clermont-Dauphin, C., Agbohessou, Y., Sanou, J., Koala, J., Faye, E., Sambakhe, D., Jourdan, C., Le Maire, G., Tall, L., Sanogo, D., Seghieri, J., Cournac, L., and Leroux, L.: How far does the tree affect the crop in agroforestry? New spatial analysis methods in a Faidherbia parkland, Agric. Ecosyst. Environ., 296, 106928, https://doi.org/10.1016/j.agee.2020.106928, 2020.

Rubio-Delgado, J., Schnabel, S., Burgess, P. J., and Burbi, S.: Reduced grazing and changes in the area of agroforestry in Europe, Front. Environ. Sci., 11, 1258697, https://doi.org/10.3389/fenvs.2023.1258697, 2023.

Rubio-Delgado, J., Schnabel, S., Lavado-Contador, J. F., and Schmutz, U.: Small woody features in agricultural areas: Agroforestry systems of overlooked significance in Europe, Agric. Syst., 218, 103973, https://doi.org/10.1016/j.agsy.2024.103973, 2024.

Sharma, P., Bhardwaj, D. R., Singh, M. K., Nigam, R., Pala, N. A., Kumar, A., Verma, K., Kumar, D., and Thakur, P.: Geospatial technology in agroforestry: status, prospects, and constraints, Environ. Sci. Pollut. Res., 30, 116459–116487, https://doi.org/10.1007/s11356-022-20305-y, 2022.

Sileshi, G. W.: The magnitude and spatial extent of influence of Faidherbia albida trees on soil properties and primary productivity in drylands, J. Arid Environ., 132, 1–14, https://doi.org/10.1016/j.jaridenv.2016.03.002, 2016.

Tahiri, O., Beillouin, D., Dumas, P., Prudhomme, R., and Makowski, D.: Classification of agroforestry systems by photo-interpretation of satellite imagery and application to quantify above-ground carbon density, Research Square [Preprint], https://doi.org/10.21203/rs.3.rs-7961411/v1, 20 May 2026.

Terasaki Hart, D. E., Yeo, S., Almaraz, M., Beillouin, D., Cardinael, R., Garcia, E., Kay, S., Lovell, S. T., Rosenstock, T. S., Sprenkle-Hyppolite, S., Stolle, F., Suber, M., Thapa, B., Wood, S., and Cook-Patton, S. C.: Priority science can accelerate agroforestry as a natural climate solution, Nat. Clim. Change, 13, 1179–1190, https://doi.org/10.1038/s41558-023-01810-5, 2023.

Tolan, J., Yang, H.-I., Nosarzewski, B., Couairon, G., Vo, H. V., Brandt, J., Spore, J., Majumdar, S., Haziza, D., Vamaraju, J., Moutakanni, T., Bojanowski, P., Johns, T., White, B., Tiecke, T., and Couprie, C.: Very high resolution canopy height maps from RGB imagery using self-supervised vision transformer and convolutional decoder trained on aerial lidar, Remote Sens. Environ., 300, 113888, https://doi.org/10.1016/j.rse.2023.113888, 2024.

UNEP-WCMC: User Manual for the World Database on Protected Areas and world database on othereffective area-based conservation measures: 1.6. UNEP-WCMC, 2019.

https://doi.org/10.5194/egusphere-2026-3696
Preprint. Discussion started: 2 July 2026

714 Vaupel, A., Bednar, Z., Herwig, N., Hommel, B., Moran-Rodas, V. E., and Beule, L.: Tree-
715 distance and tree-species effects on soil biota in a temperate agroforestry system, Plant Soil,
716 487, 355–372, https://doi.org/10.1007/s11104-023-05932-9, 2023.

717 Williams, B. A., Venter, O., Allan, J. R., Atkinson, S. C., Rehbein, J. A., Ward, M., Di Marco,
718 M., Grantham, H. S., Ervin, J., Goetz, S. J., Hansen, A. J., Jantz, P., Pillay, R., Rodríguez-
719 Buriticá, S., Supples, C., Virnig, A. L. S., and Watson, J. E. M.: Change in Terrestrial Human
720 Footprint Drives Continued Loss of Intact Ecosystems, One Earth, 3, 371–382,
721 https://doi.org/10.1016/j.oneear.2020.08.009, 2020.

722 Wu, Q.: geemap: A Python package for interactive mapping with Google Earth Engine, J.
723 Open Source Softw., 5, 2305, https://doi.org/10.21105/joss.02305, 2020.

724 Zanaga, D., Van De Kerchove, R., De Keersmaecker, W., Souverijns, N., Brockmann, C.,
725 Quast, R., Wevers, J., Grosu, A., Paccini, A., Vergnaud, S., Cartus, O., Santoro, M., Fritz,
726 S., Georgieva, I., Lesiv, M., Carter, S., Herold, M., Li, L., Tsendbazar, N.-E., Ramoino, F.,
727 and Arino, O.: ESA WorldCover 10 m 2020 v100 (v100), Zenodo [data set],
728 https://doi.org/10.5281/ZENODO.5571936, 2021.

729 Zanaga, D., Van De Kerchove, R., Daems, D., De Keersmaecker, W., Brockmann, C.,
730 Kirches, G., Wevers, J., Cartus, O., Santoro, M., Fritz, S., Lesiv, M., Herold, M., Tsendbazar,
731 N.-E., Xu, P., Ramoino, F., and Arino, O.: ESA WorldCover 10 m 2021 v200 (v200), Zenodo
732 [data set], https://doi.org/10.5281/ZENODO.7254221, 2022.

733 Zhu, X., Liu, W., Chen, J., Bruijnzeel, L. A., Mao, Z., Yang, X., Cardinael, R., Meng, F.-R.,
734 Sidle, R. C., Seitz, S., Nair, V. D., Nanko, K., Zou, X., Chen, C., and Jiang, X. J.: Reductions
735 in water, soil and nutrient losses and pesticide pollution in agroforestry practices: a review of
736 evidence and processes, Plant Soil, 453, 45–86, https://doi.org/10.1007/s11104-019-04377-
737 3, 2020.

738 Zomer, R., Trabucco, A., Coe, R., and Place, F.: Trees on Farm: Analysis of Global Extent
739 and Geographical Patterns of Agroforestry., ICRAF, Nairobi, Kenya, 2009.

740 Zomer, R. J., Trabucco A, Coe, R., Place, F., Van Noordwijk, M., and Xu, J. C.: Trees on
741 farms: an update and reanalysis of agroforestry's global extent and socio-ecological
742 characteristics, World Agroforestry Centre (ICRAF), https://doi.org/10.5716/WP14064.PDF,
743 2014.

744 Zomer, R. J., Bossio, D. A., Trabucco, A., Noordwijk, M. V., and Xu, J.: Global carbon
745 sequestration potential of agroforestry and increased tree cover on agricultural land, Circ.
746 Agric. Syst., 2, 1–10, https://doi.org/10.48130/CAS-2022-0003, 2022.

747